ACS SyntheticBiology

Research Article

pubs.acs.org/synthbio

Taking Control over Control: Use of Product Sensing in Single Cells to Remove Flux Control at Key Enzymes in Biosynthesis Pathways

Georg Schendzielorz,[†] Martin Dippong,[†] Alexander Grünberger,[†] Dietrich Kohlheyer,[†] Ayako Yoshida,[‡] Stephan Binder,[†] Chiharu Nishiyama,[‡] Makoto Nishiyama,[‡] Michael Bott,[†] and Lothar Eggeling*[,†]

[†]Institute of Bio- and Geosciences 1: Biotechnology, Forschungszentrum Jülich, D-52428 Jülich, Germany

[‡]Biotechnology Research Center, The University of Tokyo, 1-1-1 Yayoi, Bunkyo-ku, Tokyo 113-8657, Japan

Supporting Information

ABSTRACT: Enzymes initiating the biosynthesis of cellular building blocks are frequently inhibited by the end-product of the respective pathway. Here we present an approach to rapidly generate sets of enzymes overriding this control. It is based on the *in vivo* detection of the desired end-product in single cells using a genetically encoded sensor. The sensor transmits intracellular product concentrations into a graded optical output, thus enabling ultrahigh-throughput screens by FACS. We randomly mutagenized plasmid-encoded ArgB of *Corynebacterium glutamicum* and screened the library in a strain carrying the sensor pSenLys-Spc, which detects L-lysine, L-arginine and L-histidine. Six of the resulting *N*-acetyl-L-glutamate kinase proteins were further developed and characterized and found to be at least 20-fold less sensitive toward L-arginine inhibition than the wild-type enzyme. Overexpression of the mutein ArgB-K47H-V65A in *C. glutamicum*Δ*argR* led to the accumulation of 34 mM L-arginine in the culture medium. We also screened mutant libraries of *lysC*-encoded aspartate kinase and *hisG*-encoded ATP phosphoribosyltransferase. We isolated 11 LysC muteins, enabling up to 45 mM L-lysine accumulation, and 13 HisG muteins, enabling up to 17 mM L-histidine accumulation. These results demonstrate that *in vivo* screening of enzyme libraries by using metabolite sensors is extremely well suited to identify high-performance muteins required for overproduction.

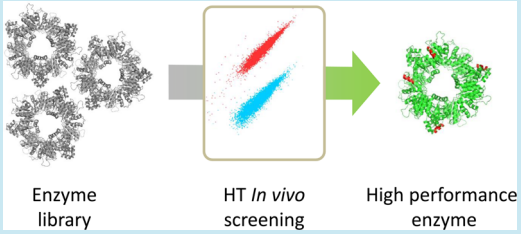

KEYWORDS: *single-cell analysis, metabolite sensor, library screening, flux control, allosteric enzymes, product sensing, fluorescence-activated cell sorting (FACS)*

The potential of microbes to convert inexpensive sugar feedstocks into industrially important products has been used for decades.[1] Vitamins, antibiotics, nucleotides, amino acids and organic acids are produced in ever increasing quantities. This biosynthetic capacity is also increasingly being used for the synthesis of small molecules not naturally made by bacteria, such as pharmaceutical intermediates or biofuels.[2,3] Examples of already established processes include the current annual production of approximately 35 tons of cobalamine, 38 000 tons of nucleotides, or as much as 5 000 000 tons of amino acids.[4] This is done using mutant strains derived from bacteria like *Propionibacterium freudenreichii*, *Escherichia coli*, or *Corynebacterium glutamicum*, for instance.

Microorganisms are not naturally designed for profitable metabolite formation, however, and there is an unrelenting need to optimize strains and pathways. Among others the catalytic activities in the biosynthesis pathway itself have to be increased to enhance and maximize the flux toward the desired metabolite. Key roles are played by enzymes that are controlled by allosteric mechanisms.[5,6] The reason for this is that such enzymes are often inhibited by the final product of the pathway or by intermediates required for its synthesis. Inhibition constants for such enzymes are often in the μM range making them unsuitable for high level production of the desired metabolite.[7] It is therefore a primary goal of many systemic engineering attempts to overcome this limitation. Unfortunately, the accessibility of deregulated enzymes is limited, and most of the engineering approaches rely on the corresponding genes derived from mutants obtained by rounds of random mutation and screening. For example, for a recent construction of a superior L-threonine producer of *E. coli* three such genes (lysC-T432I, thrA-S345F and tdh-S97F) were taken from classical mutants to enable increased flux toward L-threonine.[8] Also an L-lysine producer of *C. glutamicum* generated was based on two genes of this type (pyc-P485S, lysC-T311I) derived from classical mutants,[9] and the construction of a muconic acid producer of *Saccharomyces cerevisiae* required the use of an already available aro4-K229L allele.[10] There are other approaches to overcome allosteric inhibition and the use of the corresponding enzymes, including approaches based on crystal structures, or *in silico* predictions using coevolutionary analysis.[11,12] These latter *in vitro* approaches require plasmid constructions and screens for enzyme activity and control before they can be used. This is not the case for those enzymes obtained from *in vivo* screens, which per se are suitable for

Received: May 20, 2013
Published: July 5, 2013

   dx.doi.org/10.1021/sb400059y | *ACS Synth. Biol.* 2014, 3, 21−29

production. Easier access and a larger choice of such enzymes would be beneficial for metabolic engineering.

We recently used transcription factors and their target promoters as genetic switches to monitor increased concentrations of specific amino acids in single cells of *E. coli* or *C. glutamicum*.[13−15] The sensors developed transmit the inconspicuous phenotype of a metabolite into an easily detectable and highly sensitive optical output. This single-cell technology enables ultrahigh-throughput screens of mutant libraries since it is not restricted to colony color formation or the screening of culture supernatants by chromatography, for instance. It bridges the gap between the numerous and well-developed methods for generating large, diverse genotypic libraries on the one hand,[16] and previous less universal identification procedures for metabolite producers on the other hand. Here we apply the metabolite sensor pSenLys-Spc for the rapid identification of collections of allosterically controlled enzymes of *C. glutamicum* from large plasmid libraries, and we demonstrate their use for product formation.

RESULTS AND DISCUSSION

Monitoring Cytosolic L-Arginine in Single Cells. The metabolite sensor pSenLys-Spc, used in this study, is based on the transcriptional regulator LysG (Figure 1). The regulator

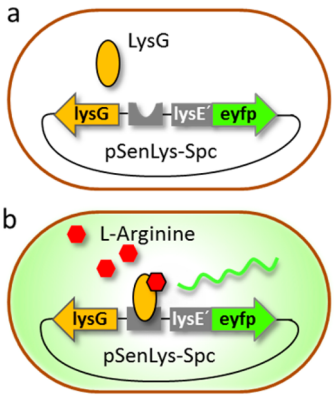

Figure 1. Principle of metabolite sensor pSenLys-Spc. (a) The sensor construct pSenLys-Spc encodes *lysE′* fused to *eyfp*. LysG is the transcriptional activator of *lysE*. (b) LysG senses elevated concentrations of L-arginine, L-lysine or L-histidine and interacts with the target promoter region to drive transcription of *eyfp* resulting in fluorescent cells.

senses increased intracellular concentrations of basic amino acids in *C. glutamicum* and drives at increased cytosolic concentrations the transcription of its target gene *lysE*.[17] In pSenLys-Spc the target promoter is fused to *eyfp*.[13]

We simulated an increased L-arginine concentration by adding the peptide Arg-Ala and followed fluorescence of single cells in a microfluidic chip over time. Peptide addition is a proven method to increase the cytosolic pool of a specific amino acid in *C. glutamicum* or *E. coli*.[18,17] Wild-type cells (WT) carrying pSenLys-Spc received 2 mM Arg-Ala in the medium feed or 2 mM Ala-Ala for control. Already after 1.25 h, cells that received the arginine-containing peptide were well separated from the control. More than 150 cells of the approximately 300 cells analyzed exhibited maximum fluorescence of 50 AU, as given by the red bars (the green bars are the control). As a further control we used *C. glutamicum* with a chromosomal deletion of the basic amino acid exporter region, WTΔlysEG. Such cells are unable to excrete L-arginine or L-lysine from the cell, and L-arginine may increase in the cytosol up to concentrations exceeding 800 mM because of the cell's inability to control the intracellular L-arginine concentration by export.[19] When WTΔlysEG received 2 mM Arg-Ala, cells exhibited the expected strong fluorescence (blue bars). In Figure 2b microscopic snapshots of 2−3 individual cells at each analyzed time point are given. For the purpose of this study it is important that, even with WT, which actively exports basic amino acids, a constant fluorescence signal prevails for Arg-Ala addition, indicating the applicability of pSenLys-Spc to identify cells with increased L-arginine synthesis due to an annulled pathway control. To see Figure 2b in time lapse, watch Video S1 (Supporting Information).

Generation and FACS Screening of ArgB Muteins. In bacteria like *C. glutamicum*, the activity of the *argB*-encoded *N*-acetyl-L-glutamate kinase is strongly inhibited by L-arginine.[20,21] The kinase initiates the L-arginine biosynthesis pathway, and control at this step prevents increased L-arginine formation. The *argB* coding sequence of *C. glutamicum* was amplified using the Diversify PCR Random Mutagenesis Kit (Clontech) to introduce 4.8 mutations per gene. The resulting library of approximately 10^5 clones was established in *E. coli* strain Top10. Transformants were pooled, plasmid DNA was isolated, and the library was introduced into *C. glutamicum*ΔargR carrying the sensor plasmid pSenLys-Spc. This latter strain was chosen since deletion of the transcriptional regulator *argR* favors L-arginine synthesis.[5] Prior to screening via FACS, cells were grown for 4 h on salt medium CGXII-glucose, as were controls containing wild-type *argB* and a control containing a known mutant *argB** allele, which is not inhibited by L-arginine.[5] Samples were gated first by electronic forward and side scatter to exclude debris, and then by fluorescence due to arginine-dependent *eyfp* transcription. The positive control was well separated from the negative control as illustrated by gate P1, which captured 0.057% of the negative control and 80.7% of the positive control (Figure 3). For selection the more stringent gate P2 was used, which captured no cell of the negative control, 0.8% of the positive control, and less than 0.001% of mutant library. About 22^6 cells of the mutant library were analyzed, and 96 positive cells were selected. These were directly spotted into 200 μL of minimal medium CGXII-glucose in a microtiter plate, and 88 of these cells grew up into cultures.

Next, the verification step was performed, and amino acids were determined in culture supernatants. In 41 cultures, L-arginine concentrations ranging from 1 to 18 mM were present, whereas in the remaining cultures up to 3 mM L-lysine was found. With the control neither L-arginine nor L-lysine was present. For unknown reasons from large populations weak L-lysine producers can easily be isolated, which is not the case for L-arginine producers. Since L-lysine elicits response of the reporter system, too, this causes the false positives. Twenty-two clones showing L-arginine accumulation to different degree were chosen, and *argB* was sequenced. Seven singular clones were obtained (Figure 4a and Table S1, Supporting Information). They differ in L-arginine accumulation and mutations in *argB*, with some clones sharing identical mutations as is typical for error-prone PCR.[16]

The significant L-arginine formation achieved by our FACS selection procedure with ArgB-14, ArgB-88, ArgB-79 and ArgB-37 encouraged us to analyze their mutations in more detail. To do so, we applied site-saturation mutagenesis individually to

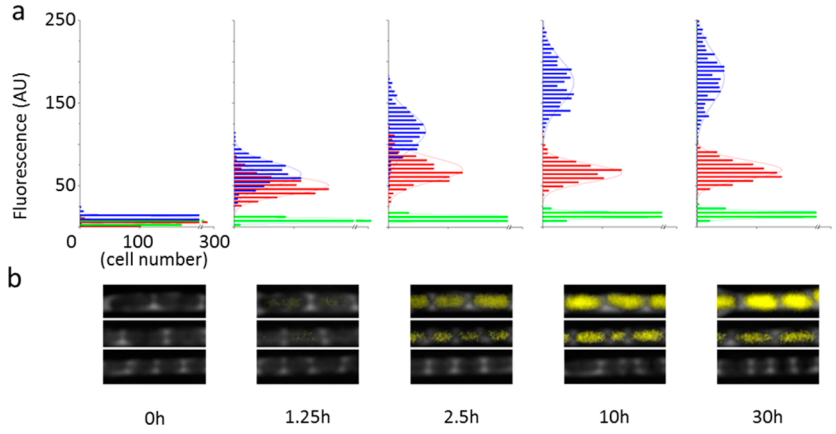

Figure 2. Fluorescence of single *C. glutamicum* cells carrying pSenLys-Spc as triggered by peptide addition. (a) At time 0 h, cells of the wild type received 2 mM Ala-Ala (green bars), or 2 mM Arg-Ala (red bars). Also strain WTΔlysEG deleted of the basic amino acid export carrier that received 2 mM Arg-Ala was used (blue bars). The fluorescence for approximately 300 cells was quantified for each time point (0−30 h). After 1.25 h, cells of the wild type that received Arg-Ala are well separated from cells that received Ala-Ala. The mutant WTΔlysEG with hampered amino acid export developed the strongest fluorescence. (b) Examples of micrographs used for quantification, each showing 2−3 cells of WTΔlysEG + Arg-Ala (top), WT + Arg-Ala (middle), and WT + Ala-Ala (bottom).

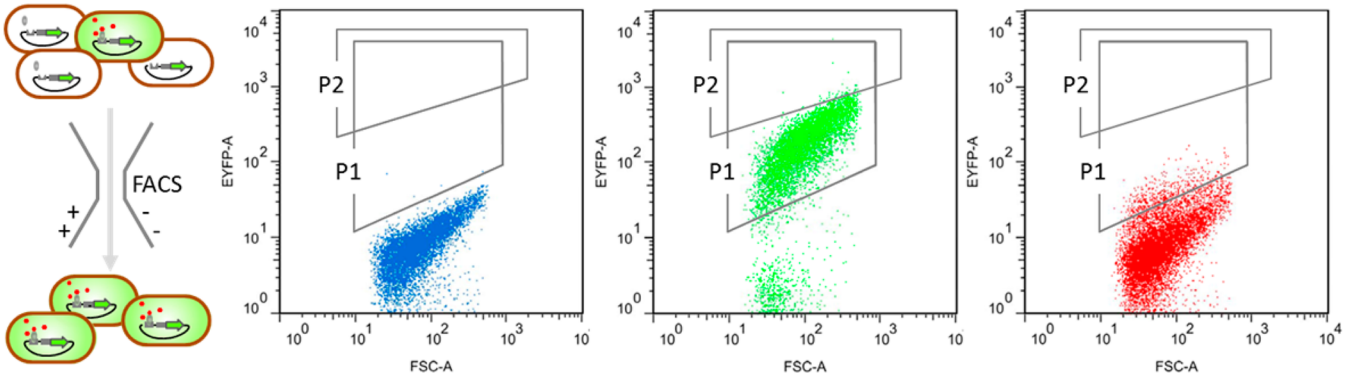

Figure 3. FACS selection of single cells with increased cytosolic L-arginine concentration. On the left, a sketch of the FACS selection procedure is shown. The three FACS plots illustrate, from left to right, the negative control with wild-type *argB*, the positive control with cells expressing the mutant *argB** allele, and cells containing the error-prone PCR library of *argB*. The stringent gate P2 was used for selection.

K47, V65, V110, G122, T180, I189, Y190 (Table S2, Supporting Information) and selected fluorescent cells via FACS from each of the seven libraries as described before. In the case of the G122 library, we isolated a single mutein, ArgB-G122T, and obtained a top L-arginine accumulation of 11.5 ± 0.3 mM (see Table S3, Supporting Information). Moreover, interesting muteins were selected from the assay where K47 was saturated. Strains with ArgB muteins K47E, K47T and K47H produced 1.2, 3.5, and 5.5 mM L-arginine, respectively, whereas with wild-type ArgB, 0.4 mM L-arginine was obtained. Residue K47 of *C. glutamicum* aligns with the corresponding K/R residues of the ArgB proteins of *Mycobacterium tuberculosis*, *Pseudomonas aeruginosa*, *Arabidopsis thaliana*, and *Thermotoga maritima* with known structure (Figure S5, Supporting Information). In these structures, the respective K/R residues are in the αA helix (Figure 4b), which is connected via the β1 strand to the N-terminal helix whose complete deletion abolished L-arginine inhibition of the *P. aeruginosa* enzyme.[23] In the model for the *C. glutamicum* enzyme, K47 is only able to interact with the amide backbone of V42 (3.1 Å). However, K47H is also able to interact with the amide backbone of residues D43 and D44 (<3.5 Å) and the side-chain of Y36 (3.6 Å). These slight alterations might impact on the overall structural organization of the preceding β1 strand and thus affect L-arginine sensitivity via the N-terminal helix. For further development of ArgB we focused on positions K47 and V65 because of the highest production obtained with this mutein. We combined with these mutations a limited set of further mutations by site-directed mutagenesis. In total 6 mutants were generated whose production properties and enzymatic properties were explored in more detail (Table 1). In particular, the combination of K47H with V65A gave rise to an enzyme that caused an exceptionally high L-arginine concentration, whereas further combination with G122T led to a reduction again. Thus upon combining K47H with V65A, an additive effect was present, as occasionally observed for nearby changes in enzyme development.[24]

Kinetic and Physical Characterization of ArgB Muteins. We were also interested in selected biochemical parameters of the obtained ArgB muteins. To this end, the muteins were isolated as His-tagged versions from *E. coli*, and kinetic characteristics were determined. As expected, ArgB-WT was inhibited at low L-arginine concentrations characterized by a K_i of 0.2 mM (Table 2). This agrees with prior work reporting that the enzyme of *C. glutamicum* is inhibited to half its activity by 0.4−2 mM L-arginine.[25,21] All muteins analyzed exhibited an at least 19.5-fold reduced sensitivity toward the allosteric inhibitor L-arginine.

dx.doi.org/10.1021/sb400059y | *ACS Synth. Biol.* 2014, 3, 21−29

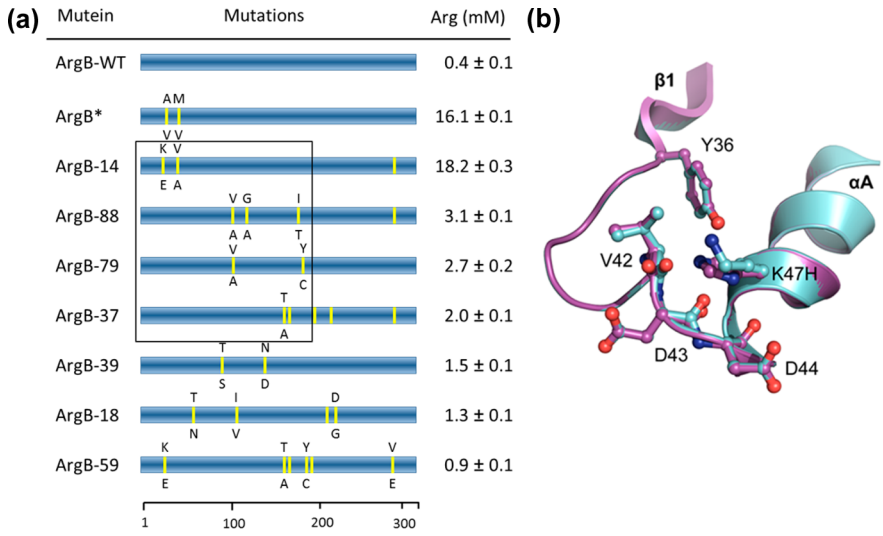

Figure 4. (a) Mutations of the isolated ArgB muteins and the L-arginine accumulation they cause. The yellow bar indicates the approximate location of the mutation. In the case of an amino acid exchange, the WT amino acid is given on top and the mutant amino acid below the yellow bar. The mutant locations that were studied in more detail are framed (see text). (b) Structural overlay of aa 32−53 of ArgB-WT (cyan) and ArgB-K47H (magenta) generated by SWISS-MODEL.[22] The histidine residue in position 47 is able to interact with the amide backbone of residues D43 and D44 and the side-chain of Y36, which results in a slight distortion of the αA helix and the preceding β1 strand, which may influence the degree of L-arginine sensitivity.

Table 1. Influence of Overproduction of Selected ArgB Muteins and Wild-Type ArgB in *C. glutamicum*Δ*argR* on L-Arginine Accumulation in Culture Supernatants[a]

mutation	L-arginine (mM)
No	0.4 ± 0.1
K47H	8.3 ± 0.9
K47H, V65A	34.9 ± 1.2
K47H, V65A, G122T	22.2 ± 2.7
K47H, V65A, T180P	32.5 ± 1.4
K47H, G122T	12.4 ± 0.8
K47H, G122T, T180P	10.1 ± 0.9

[a]Strains were grown for 48 h in minimal medium CGXII-glucose.

ArgB-K47H-V65A is most interesting with respect to its impact on L-arginine production. This enzyme has an intermediate K_i among the isolated muteins, and it retains a reasonable catalytic efficiency of 1.1 s^{-1} mM^{-1} (Table 2). High L-arginine concentrations were also obtained with ArgB-K47H-V65A-T180P and ArgB-K47H-V65A-G122T. The latter protein was obtained from *E. coli* in very low yields only and was not further analyzed. The comparison of ArgB-K47H-G122T and ArgB-K47H-G122T-T180P is informative. These two proteins differ greatly with respect to catalytic efficiency, but perform similarly with respect to product accumulation. This emphasizes the advantage of the *in vivo* selection of productive enzymes, because *in vitro* derived kinetic characterizations apparently do not integrate the total cellular characteristics required for overproduction.

The *N*-acetyl-L-glutamate kinase of *E. coli* is a dimer, and it is not inhibited by L-arginine,[21] whereas the enzyme of *Pseudomonas aeruginosa* and *Thermotoga maritima* is a hexamer and is sensitive toward L-arginine inhibition.[20] For the *P. aeruginosa* enzyme, there are indications that the global structure of the protein displays slight structural alterations during conversion from the relaxed to the tensed state upon interaction with the inhibitor.[26,20] We therefore studied the consequences of L-arginine addition on the *C. glutamicum* enzyme by size exclusion chromatography (Figure 5). As expected from the sequence, the wild-type enzyme eluted with an apparent mass of 231 ± 40 kDa, which indicates that the enzyme is a hexamer (6 × 34.88 kDa = 209 kDa). In the presence of 10 mM L-arginine, the elution profile was almost superimposable (blue line in Figure 5). The elution profiles for the ArgB-K47H-G122T-T180P and ArgB-K47H-V65A enzymes were very different. Without L-arginine present, ArgB-K47H-G122T-T180P eluted in the void volume, which suggests that the mutations promote a high oligomeric state exceeding that of a hexamer. However, in the presence of L-arginine, the protein eluted according to a hexamer (Table S4,

Table 2. Kinetic Characterization of Selected Key Enzymes

protein[a]	K_m (mM)	spec. activity (μmol min^{-1} mg^{-1})	k_{cat} (s^{-1})	efficiency k_{cat}/K_m (s^{-1} mM^{-1})	K_i (mM)
ArgB-WT	3.4 ± 0.3	39.5 ± 0.9	23.0	6.8	0.2
ArgB-A49V-M54V*	2.9 ± 0.3	5.5 ± 0.1	3.2	1.1	7.0
ArgB-K47H	15.7 ± 2.1	71.1 ± 2.9	41.3	2.6	7.4
ArgB-K47H-G122T	25.3 ± 1.2	2.4 ± 0.06	1.4	0.1	3.7
ArgB-K47H-V65A	7.5 ± 0.7	14.0 ± 0.2	8.1	1.1	3.9
ArgB-K47H-G122T-T180P	5.6 ± 0.4	18.4 ± 0.3	10.6	1.9	6.9
ArgB-K47H-V65A-T180P	5.8 ± 0.6	29.5 ± 0.5	17.1	2.9	11.5

[a]The ArgB-A49V-M54V* protein has already been described.[5] The yield of ArgB-K47H-V65A-G122T was too low to enable its detailed analysis.

dx.doi.org/10.1021/sb400059y | *ACS Synth. Biol.* 2014, 3, 21−29

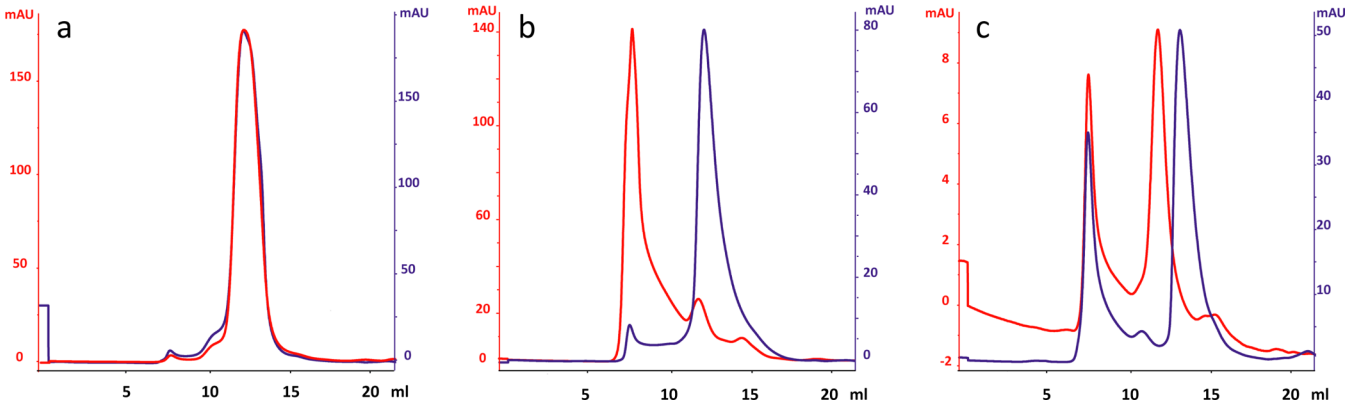

Figure 5. Structural alterations of ArgB proteins in the presence or absence of L-arginine. Three different proteins were subjected to size exclusion chromatography in the absence (red) or presence (blue) of 10 mM L-arginine: (a) ArgB-WT; (b) ArgB-K47H-G122T-T180P; (c) ArgB-K47H-V65A.

Table 3. Overview of LysC and HisG Muteins Obtained by Direct Product Sensing Using Metabolite Sensor Technology[a]

protein							L-lysine (mM)
LysC-WT							1.2 ± 0.1
LysC-77	R20S	N21D	T311I	R399L			44.9 ± 1.5
LysC-88	N21D	T311I					44.8 ± 1.1
LysC-90	N21D	L125L	E278G	A280V			39.0 ± 0.7
LysC-63	L69F	A124P	I211V	L227P	N235D	V350A	32.5 ± 0.7
LysC-56	K141K	V159E	N337S	D341N			30.9 ± 5.3
LysC-57	N21D	M365K	L394L				29.5 ± 0.3
LysC-15	N21D	T311I	R399L				27.1 ± 1.6
LysC-2	N21D	L125L	E278G	A280V	E391G		24.9 ± 2.4
LysC-54	T311I						23.9 ± 2.5
LysC-8	E24G	T311I					23.0 ± 0.1
LysC-42	R20S	N21D	N78S	E123E	I186V	K328E	21.1 ± 1.2
protein							L-histidine (mM)
HisG-WT							0.0
HisG-GT233-3	G233H	T235Q					17.3 ± 1.1
HisG-GT233-8	G233S	T235R					15.3 ± 0.2
HisG-GT233-4	G233V	T235R					14.7 ± 0.1
HisG-GT233-5	G233I	T235V					14.3 ± 0.3
HisG-GT233-1	G233R	T235R					13.4 ± 0.7
HisG-GT233-10	G233L						13.2 ± 0.4
HisG-GT233-6	G233H	T235F					13.1 ± 0.5
HisG-GT233-11	G233P	T235L					11.4 ± 0.5
HisG-GT233-7	G233R						10.7 ± 0.4
HisG-GT233-2	G233S	T235H					9.5 ± 0.5
HisG-N216-1	N216I						12.5 ± 0.2
HisG-N216-3	N216R						12.4 ± 1.2

[a]The *lysC* alleles were derived by epPCR. The *hisG* alleles resulted from applying two saturating primer sets: one targeting codon 233 and codon 235, and the other targeting codon 216. See Tables S6 and S7 (Supporting Information) for nucleotide exchanges.

Supporting Information). For ArgB-K47H-V65A, apparently three different globular structures can be formed: a large one eluting in the void volume, an intermediate one according to a hexamer, and a small one with an elution volume below a hexamer, which could be a tetramer or a dimer. L-arginine shifted the intermediate form to the small form. This shows that exceptional structural alterations of the *N*-acetyl-L-glutamate kinase are possible, which apparently do not result in a substantial loss of activity and efficiency (Table 2), and which are most useful for production purposes (Table 1). The hexameric kinase proteins have an extra N-terminal helix, which interlinks three dimers in the hexamers.[20] As previously mentioned K47 and V65 are located in the αA-helix (Figure 4b), and the observed insensitivity of ArgB-K47H-V65A toward L-arginine is apparently related with the dissociation of the hexamer into active smaller aggregates, as was similarly observed for mutant enzymes of *P. aeruginosa*.[23]

Generation of LysC and HisG Muteins. As mentioned earlier, the metabolite sensor based on the transcriptional regulator LysG detects L-arginine, L-lysine and L-histidine.[13] Its successful use to identify L-arginine-insensitive ArgB muteins prompted us to apply the same approach to screen mutant libraries for deregulated key enzymes of L-lysine and L-histidine synthesis, respectively. The key enzyme of L-lysine synthesis in *C. glutamicum* is the aspartate kinase (LysC), which is inhibited in its activity by L-lysine,[27] whereas the ATP phosphoribosyl-

dx.doi.org/10.1021/sb400059y | *ACS Synth. Biol.* 2014, 3, 21−29

transferase (HisG) controls L-histidine synthesis and is inhibited by L-histidine.[28] To this end, *lysC* of *C. glutamicum* was amplified by error-prone PCR, and PCR products cloned into pSenLys to give pSenLys-PlysC. Plasmids prepared from *E. coli* were pooled and used to transform *C. glutamicum*. LysC-T311I, encoding a known lysine-insensitive kinase protein,[29] served as a positive control for FACS screenings. In total 3×10^6 cells were screened and as a result, 11 different *lysC* alleles isolated. Among them, alleles with up to seven mutations were found, as was the single *lysC*-T311I mutation (Table 3). These muteins caused L-lysine accumulation up to 44.9 mM in CGXII-glucose medium. Interestingly, each of the muteins carried at least one mutation in the carboxy-terminal part of LysC corresponding to the β-region of the protein known to control kinase activity.[6] Three LysC muteins were also characterized with respect to their inhibition profile by L-lysine (Figure S7, Supporting Information). Whereas the wild type enzyme is inhibited to half of its activity at about 1 mM L-lysine, the three muteins LysC-c77, LysC-c80, and LysC-c90 are virtually uninhibited at a concentration of 10 mM L-lysine.

To mutate HisG of *C. glutamicum*, we used a slightly different approach. The structure of the homologous ATP phosphoribosyltransferase of *Mycobacterium tuberculosis* in complex with the inhibitor L-histidine suggested that specific key residues are involved in histidine binding.[30] We defined equivalent residues in the HisG structure of *C. glutamicum* by homology-modeling using SWISS-MODEL.[22] Five mutagenic primer sets were designed and used for site-saturation mutagenesis of pCLTON2-encoded *hisG* (Table S5, Supporting Information). *C. glutamicum* cells carrying pSenLys were transformed with the saturation libraries. The libraries derived from the five mutagenic primer sets were analyzed separately via FACS, and in two libraries cells with increased fluorescence were present. 48 cells from the two positive libraries were isolated and further analyzed by culture fluorescence and product quantification. Sequencing, retransformation, and product quantification confirmed that 12 different HisG muteins resulted in significant L-histidine accumulation of up to 17 mM (Table 3). Again, three muteins were isolated and assayed for their inhibition by L-histidine (Figure S7, Supporting Information). Whereas the wild type mutein is inhibited to half of its activity at a concentration of 0.2 mM L-histidine, half of the activity is still present with the mutein HisG-GT233HQ at a concentration of 15 mM L-histidine. The muteins HisG-N216R and HisG-N216I retain almost full activity even at 30 mM L-histidine. Thus, our study confirms that selected key residues proposed by Cho et al.[30] interact with the allosteric inhibitor L-histidine on the one hand and provide muteins useful for overproduction on the other hand.

With a few exceptions, so far most of the key enzymes released from feedback control and used for production originate from random mutagenesis of whole cells. Our approach offers rapid access to new alleles, a large choice of which is useful for production purposes. This is of relevance because overriding the control of initial key enzymes may be decisive for product formation, as exemplified for the aspartate kinase of *C. glutamicum*, where different alleles yielded very different L-lysine accumulations.[31,12,32] Also our data on product accumulation obtained with the different allels of *lysC*, *argB* or *hisG* support this view. Of course, our approach on *in vivo* screening using metabolite sensors relies on the availability of appropriate proteins that regulate a promoter's transcriptional output in response to a small-molecule ligand. However, such proteins are naturally at hand because the synthesis of natural products like amino acids, nucleotides, or vitamins, for instance, is controlled by transcription factors. In fact, metabolite sensors for the transformation of cytosolic metabolite concentrations into a graded optical output have already been described for metabolites like L-methionine, L-serine, L-arginine, L-leucine, mevalonate, or *O*-acetyl-serine for *C. glutamicum* and *E. coli*.[13,14,33] The development of new sensor specificities will create more opportunities for isolating enzymes that are ideally suited to the cellular requirements for product formation.

METHODS

Strains, Plasmids, and Growth Conditions. *Corynebacterium glutamicum* was grown at 30 °C either on brain heart infusion medium (Difco) or in the MOPS-buffered minerals salt medium CGXII, which contained 4% glucose as carbon source.[34] When appropriate, media contained 25 μg mL^{-1} of kanamycin or 100 μg mL^{-1} of spectinomycin. Strains and plasmids are shown in Table 4. Genes were cloned as follows:

Table 4. Strains and Plasmids Used

strain/plasmid	relevant characteristics	origin
WT	Wild type, ATCC 13032, biotin-auxotroph	Culture Collection
WTΔlysEG	Wild type deleted of *lysEG*	Vrljic et al.[19]
WTΔargR	Wild type deleted of *argR*	Staebler et al.[35]
pSenLys	Encodes LysG, and its target promoter fused to *eyfp*; KanR	Binder et al.[13]
pSenLys-Spc	Encodes LysG, and its target promoter fused to *eyfp*; SpcR	this work
pAN6	Shuttle vector; KanR	Niebisch et al.[36]
pAN6-ArgB	pAN6 with *argB* (NC_006958.1: 1467889...1468842)	this work
pSenLys-PlysC	pSenLys with *lysC* (NC_006958.1: 268851...270636)	this work
pCLTON2	Shuttle vector; SpcR derived from pCLTON1	Lausberg et al.[37]
pClTON2-hisG	pCLTON2 with *hisG* (NC_006958.1: 1467889...1468842)	this work
pUC18-argB	pUC18 with *argB* (NC_006958.1: 1467889...1468842)	this work
pUC18-lysC	pUC18 with *lysC* (NC_006958.1: 269371...270636)	this work
pET26b(+)-argB	pET26b(+) with *argB* (NC_006958.1: 1467889...1468842)	this work
pET26b(+)-lysC	pET26b(+) with *lysC* (NC_006958.1: 269371...270636)	this work
pET28b(+)-hisG	pET28b(+) with *hisG* (NC_006958.1: 1467889...1468842)	this work

argB into NdeI/EcoRI cleaved pAN6, *lysC* with its promoter region into XhoI/SalI prepared pSenLys, *hisG* into SmaI/SacI cleaved pCLTON2, *lysC* into BamHI/EcoRI cleaved pUC18, *argB* into NdeI/XhoI prepared pET26b(+), *lysC* into XhoI/NdeI cleaved pET26b(+), and *hisG* into BamHI/EcoRI digested pET28b(+). The correct integration of the inserts and their integrity were verified by sequencing.

Microfluidic Chip Cultivations and Live Cell Imaging. *Corynebacterium glutamicum* cells were inoculated from cryostocks into CGXII-glucose containing 25 μg mL^{-1} of kanamycin and incubated at 30 °C for 16 h.[34] These precultures were used to inoculate fresh cultures to an OD of

dx.doi.org/10.1021/sb400059y | ACS Synth. Biol. 2014, 3, 21−29

2, cultivated for 5 h, and then diluted to an OD of 0.5 for infusion into the chip (for the principle and design of the microfluidic single-cell chemostat, see Figure S3, Supporting Information). Subsequently, fresh CGXII-glucose was infused into the chip device at approximately 100 nL min^{-1} per channel using 1 mL syringes and high-precision syringe pumps for continuous media supply (neMESYS, Cetoni, Germany). After being grown for 20 h, CGXII-glucose supplemented with 2 mM Arg-Ala or Ala-Ala was applied (Bachem AG, Bubendorf, Switzerland).

The chip was mounted onto a motorized inverted microscope (Nikon Eclipse Ti) inside an in-house manufactured incubator for temperature and atmosphere control, as described previously.[15] Furthermore, the microscope was equipped with a focus assistant Nikon PFS compensating for thermal drift during long-term microscopy, and a heated Nikon Apo TIRF 100× Oil DIC N objective (ALA OBJ-Heater, Ala Scientific Instruments, USA). Phase contrast and fluorescence time lapse images of several cell arrays were captured every 15 min. Fluorescence images were recorded using an ANDOR LUCA R DL604 CCD camera with an exposure time of 200 ms. YFP was excited using a 300 W Xenon light source (Lamda DG-4 Sutter Instruments) at maximum intensity and using appropriate optical filters (excitation: HQ 500/20, dichroic: Q515, emission: HQ 535/30; Chroma). The settings were not changed between experiments to allow a direct comparison of fluorescence intensities. The final images were analyzed with the Nikon NIS Elements AR software package to determine cell size and fluorescence intensity. After cell division, one adjacent daughter cell was selected as the next cell of interest.

Error Prone PCR and Plasmid Library Construction. The genes *argB*, *lysC* and *hisG* were derived from genomic DNA of *C. glutamicum* ATCC13032 using KOD-polymerase (Novagen, Merck KGaA, Darmstadt, Germany). PCR products of *argB* and *lysC* were purified, digested with BamHI/EcoRI (Fermentas, Thermo Fisher Scientific, Waltham, MA, USA) and ligated into appropriately prepared pUC18. Error-prone PCR was performed using the Diversify kit (Clonetech, Saint-Germain-en-Laye, France) together with primers annealing 50 bp upstream and downstream of the target gene, respectively. Conditions were chosen to introduce between 2 and 9 mutations per kb, as given in the supplier's manual. Error prone PCR products of *argB* and *lysC* were purified and ligated via NdeI/EcoRI with pAN6 or via XhoI/SalI with pSenLys-PlysC, respectively. *hisG* PCR products were cloned via the SmaI/SacI sites into pCLTON2. Saturation libraries were constructed using QuikChange XL (Agilent, Santa Clara, CA 95051, USA) and saturating primers were ordered with NNK/MNN at the target position (LifeTechnologies GmbH, 64293 Darmstadt, Germany). The plasmids constructed are given in Figure S4 (Supporting Information). For library construction, electrocompetent *E. coli* DH5α cells were used. Cells were regenerated in LB medium and after regeneration inoculated into 15 mL of LB medium containing the appropriate antibiotic. After overnight cultivation, plasmid libraries were isolated from these cultures.

FACS and Library Screening. To enable sorting, *C. glutamicum*ΔargR pSenLys-Spc was transformed with the *argB* library in pAN6. The *lysC* library was directly established in pSenLysPlysC and used to transform *C. glutamicum* WT. The *hisG* library was established in pCLTON2 and used to transform *C. glutamicum* pSenLys. Cells were regenerated in BHI complex medium (Difco Laboratories Inc., Detroit, MI, USA) for 1 h at 30 °C and plated on BHI agar plates containing 25 μg mL^{-1} of kanamycin and 100 μg mL^{-1} of spectinomycin. Plates were incubated for 24 h at 30 °C and swept with 2 mL of CGXII-glucose.[34] The cell suspensions were stored as cryostocks containing 40% glycerol (w/v). Prior to FACS, CGXII-glucose precultures containing the appropriate antibiotics were inoculated from the cryostocks and then grown overnight, before being used to inoculate fresh cultures, which were grown up to OD 2. The culture containing the *argB* library received 1 mM IPTG, and the culture with the *hisG* library 250 ng mL^{-1} of anhydrotetracyclin. Approximately 22 ×10^6, 3 × 10^6, and 1 × 10^5 cells from strains, expressing *argB*, *lysC*, and *hisG* libraries, respectively, were subjected to the FACS analysis 4−6 h later. Cells emitting high fluorescence were spotted directly into 96 well plates, prefilled with 200 μL of CgXII and the appropriate antibiotics. Cultures grown after 48 h were further analyzed.

Immediately prior to FACS analysis, the cell suspensions were diluted to an optical density below 0.1 and analyzed by a FACS ARIA II high-speed cell sorter (BD Biosciences, Franklin Lakes, NJ, USA) using excitation/emission wavelength of 488/530 ± 20 nm and a sample pressure of 70 psi. Data were analyzed using BD DIVA 6.1.3 and FlowJo 7.6.5 software (Tree Star, Inc., Ashland, OR 97520). The electronic signal threshold was defined to exclude nonbacterial particles on the basis of forward versus side scatter areas. Electronic gating in the EYFP channel was set to exclude nonfluorescent cells. Noise level was defined by nonproducing *C. glutamicum* cells, expressing the wild-type allele of the specific target gene.

High-Throughput Cultivation and Analyses. High-throughput cultivation was done in 48-well Flowerplates (FPs; m2p-laboratories GmbH, Baesweiler, Germany) in 0.7 mL of minimal medium CGXII-4% glucose (CGXII-glucose) at 30 °C, 900 rpm and a throw of ø 3 mm. The specific geometry of the FPs ensures high mass-transfer performance and allowed them to be used together with the microcultivation system BioLector allowing online monitoring of growth and fluorescence.[38] For offline cultivations, FPs were cultivated on a Microtron high-capacity micro plate incubator operating at a shaker speed of 900 rpm and a throw of ø 3 mm (Infors AG, CH-4103 Bottmingen, Switzerland). Cells pregrown in CGXII medium were used as inocula for all cultivations. Amino acids were quantified as their *o*-phthaldialdehyde derivatives via high-pressure liquid chromatography as their fluorescent isoindole derivatives, as previously described.[13]

Protein Work. *N*-Acetyl-L-glutamate kinase (*argB*) and aspartate kinase (*lysC*) encoding genes were cloned into pET26b(+) via NdeI/XhoI or BamHI/EcoRI, respectively. Phosphoribosyl transferase encoding genes (*hisG*) were cloned into pET28b(+) via XhoI/NdeI. *E. coli* Bl21(DE3) was transformed with these plasmids and inoculated into 5 mL 2xYT. These precultures were used to inoculate fresh 2xYT (1:100) cultures, which were incubated for 3 h at 37 °C. IPTG was added (1 mM), and they were further incubated for 16 h at 25 °C. Cells were harvested, washed and disrupted in sonication buffer 20 mM Tris-HCl pH7.5, 150 mM NaCl (Branson Ultrasonics Corporation, Danbury, CT, USA). Crude extract supernatants derived from centrifugation (50 000 rpm, 4 °C, 1 h) were applied to Ni-NTA columns, and protein was eluted as recommended by the manufacturer (Qiagen, Hilden, Germany). Elution fractions were analyzed by SDS-PAGE, and concentrated using Amicon Ultra-4 30K centrifugal filters (Millipore Corporation, Billerica, MA01821).

Gel filtrations were performed on an Äkta-P900 System (GE Healthcare, Buckinghamshire, UK) equipped with a Superdex 200 10/300 GL column buffered in 20 mM HEPES, 150 mM NaCl, ± 10 mM L-arginine. UV absorbance was detected with a UPC-900 module, and data were analyzed with the Unicorn 5.01 software (Amersham Biosciences, Amersham, UK). The *N*-acetyl-L-glutamate kinase and aspartate kinase activity was essentially assayed as described by Haas and Leisinger[26] and Black and Wright,[39] respectively. Both are based on complex formation of the synthesized *N*-acetylglutamyl-phosphate or aspartyl-phosphate with Fe^{3+} ions and were scaled down for our purpose to a volume of 100 μL and performed in microtiter plates. Complex formation was determined at 540 nm (ε = 456 M^{-1} cm^{-1}). The phosphoribosyl transferase activity was essentially assayed as described by Ames.[40] Conditions were scaled down to a volume of 150 μL and performed in microtiter plates. Product formation was detected at 290 nm (ε = 3600 M^{-1} cm^{-1}).

Structure Modeling. Structural models of the *C. glutamicum* ArgB and ArgB-K47H were generated with SWISS-MODEL using the structural template of *P. aeruginosa* (PDB ID: 2BUF).

■ ASSOCIATED CONTENT

Supporting Information

A video showing fluorescence development in single cells. Figure S1 gives the dose−response curve of peptide addition. Figure S2 shows the microfluidic device used. Figure S3 shows the plasmids used. Figure S4 gives isothermal titration calorimetry information. Figure S5 shows the sequence alignments of different ArgB genes. Figure S6 gives selected inhibition kinetics for LysC and HisG proteins. Furthermore, tables are included giving the nucleotide exchanges of the alleles obtained and data on gel filtrations. This material is available free of charge via the Internet at http://pubs.acs.org.

■ AUTHOR INFORMATION

Corresponding Author

*E-mail: l.eggeling@fz-juelich.de.

Author Contributions

G.S., M.D., A.G., A.Y., and S.B. performed the experiments, D.K., M.N., C.N., and M.B. provided guidance for experimental set-ups, and L.E. and G.S. wrote the paper.

Notes

The authors declare no competing financial interest.

■ ACKNOWLEDGMENTS

The authors thank Marcus Schallmey for assistance interpretating the ArgB mutations. Support from the BMBF Grant 0315589A "Corynebacterium: improving flexibility and fitness for industrial production" is gratefully acknowledged.

■ REFERENCES

(1) Adrio, J. L., and Demain, A. L. (2010) Recombinant organisms for production of industrial products. *Bioeng. Bugs 1*, 116−131.

(2) Tsuruta, H., Paddon, C. J., Eng, D., Lenihan, J. R., Horning, T., Anthony, L. C., Regentin, R., Keasling, J. D., Renninger, N. S., and Newman, J. D. (2009) High-level production of amorpha-4,11-diene, a precursor of the antimalarial agent artemisinin *Escherichia coli*. *PLoS One 4*, e4489.

(3) Dunlop, M. J., Dossani, Z. Y., Szmidt, H. L., Chu, H. C., Lee, T. S., Keasling, J. D., Hadi, M. Z., and Mukhopadhyay, A. (2011) Engineering microbial biofuel tolerance and export using efflux pumps. *Mol. Syst. Biol. 7*, 487.

(4) Eggeling, L., Pfefferle, W., and Sahm, H. (2006) Amino Acids, in *Basic Biotechnology* (Radledge, C., Kristiansen, B., Eds.) pp 335−398, Cambridge University Press, Cambridge.

(5) Ikeda, M., Mitsuhashi, S., Tanaka, K., and Hayashi, M. (2009) Reengineering of a *Corynebacterium glutamicum* L-arginine and L-citrulline producer. *Appl. Environ. Microbiol. 75*, 1635−1641.

(6) Yoshida, A., Tomita, T., Kuzuyama, T., and Nishiyama, M. (2010) Mechanism of concerted inhibition of alpha2beta2-type hetero-oligomeric aspartate kinase from *Corynebacterium glutamicum*. *J. Biol. Chem. 285*, 27477−27486.

(7) Suter, P., and Rosenbusch, J. P. (1977) Asymmetry of binding and physical assignments of CTP and ATP sites in aspartate transcarbamoylase. *J. Biol. Chem. 252*, 8136−8141.

(8) Lee, K. H., Park, J. H., Kim, T. Y., Kim, H. U., and Lee, S. Y. (2007) Systems metabolic engineering of *Escherichia coli* for L-threonine production. *Mol. Syst. Biol. 3*, 149.

(9) Becker, J., Zelder, O., Hafner, S., Schroder, H., and Wittmann, C. (2011) From zero to hero—design-based systems metabolic engineering of *Corynebacterium glutamicum* for L-lysine production. *Metab. Eng. 13*, 159−168.

(10) Curran, K. A., Leavitt, J. M., Karim, A. S., and Alper, H. S. (2013) Metabolic engineering of muconic acid production in *Saccharomyces cerevisiae*. *Metab. Eng. 15*, 55−66.

(11) Hatley, M. E., Lockless, S. W., Gibson, S. K., Gilman, A. G., and Ranganathan, R. (2003) Allosteric determinants in guanine nucleotide-binding proteins. *Proc. Natl. Acad. Sci. U. S. A. 100*, 14445−14450.

(12) Chen, Z., Meyer, W., Rappert, S., Sun, J., and Zeng, A.-P. (2011) Coevolutionary analysis enabled rational deregulation of allosteric enzyme inhibition in *Corynebacterium glutamicum* for lysine production. *Appl. Environ. Microbiol. 77*, 4352−4360.

(13) Binder, S., Schendzielorz, G., Stabler, N., Krumbach, K., Hoffmann, K., Bott, M., and Eggeling, L. (2012) A high-throughput approach to identify genomic variants of bacterial metabolite producers at the single-cell level. *Genome Biol. 13*, R40.

(14) Mustafi, N., Grünberger, A., Kohlheyer, D., Bott, M., and Frunzke, J. (2012) The development and application of a single-cell biosensor for the detection of L-methionine and branched-chain amino acids. *Metab. Eng. 14*, 449−457.

(15) Grünberger, A., Paczia, N., Probst, C., Schendzielorz, G., Eggeling, L., Noack, S., Wiechert, W., and Kohlheyer, D. (2012) A disposable picolitre bioreactor for cultivation and investigation of industrially relevant bacteria on the single cell level. *Lab Chip 12*, 2060−2068.

(16) Cadwell, R. C., and Joyce, G. F. (2006) Mutagenic PCR. *CSH Protoc.*, DOI: 10.1101/pdb.prot4143 .

(17) Bellmann, A., Vrljic, M., Pátek, M., Sahm, H., Krämer, R., and Eggeling, L. (2001) Expression control and specificity of the basic amino acid exporter LysE of *Corynebacterium glutamicum*. *Microbiology 147*, 1765−1774.

(18) Tavori, H., Kimmel, Y., and Barak, Z. (1981) Toxicity of leucine-containing peptides in *Escherichia coli* caused by circumvention of leucine transport regulation. *J. Bacteriol. 146*, 676−683.

(19) Vrljic, M., Sahm, H., and Eggeling, L. (1996) A new type of transporter with a new type of cellular function: L-lysine export from *Corynebacterium glutamicum*. *Mol. Microbiol. 22*, 815−826.

(20) Ramon-Maiques, S., Fernandez-Murga, M. L., Gil-Ortiz, F., Vagin, A., Fita, I., and Rubio, V. (2006) Structural bases of feed-back control of arginine biosynthesis, revealed by the structures of two hexameric *N*-acetylglutamate kinases, from *Thermotoga maritima* and *Pseudomonas aeruginosa*. *J. Mol. Biol. 356*, 695−713.

(21) Xu, Y., Labedan, B., and Glansdorff, N. (2007) Surprising arginine biosynthesis: a reappraisal of the enzymology and evolution of the pathway in microorganisms. *Microbiol. Mol. Biol. Rev. 71*, 36−47.

(22) Arnold, K., Bordoli, L., Kopp, J., and Schwede, T. (2006) The SWISS-MODEL workspace: a web-based environment for protein structure homology modelling. *Bioinformatics 22*, 195−201.

(23) Fernandez-Murga, M. L., and Rubio, V. (2008) Basis of arginine sensitivity of microbial *N*-acetyl-L-glutamate kinases: mutagenesis and protein engineering study with the *Pseudomonas aeruginosa* and *Escherichia coli* enzymes. *J. Bacteriol. 190*, 3018−3025.
(24) Bornscheuer, U. T., Huisman, G. W., Kazlauskas, R. J., Lutz, S., Moore, J. C., and Robins, K. (2012) Engineering the third wave of biocatalysis. *Nature 485*, 185−194.
(25) Sakanyan, V., Petrosyan, P., Lecocq, M., Boyen, A., Legrain, C., Demarez, M., Hallet, J. N., and Glansdorff, N. (1996) Genes and enzymes of the acetyl cycle of arginine biosynthesis in *Corynebacterium glutamicum*: enzyme evolution in the early steps of the arginine pathway. *Microbiology 142*, 99−108.
(26) Haas, D., and Leisinger, T. (1975) *N*-Acetylglutamate 5-phosphotransferase of *Pseudomonas aeruginosa*. Purification and ligand-directed association-dissociation. *Eur. J. Biochem. 52*, 365−375.
(27) Shiio, I., Miyajima, R., and Sano, K. (1970) Genetically desensitized aspartate kinase to the concerted feedback inhibition in *Brevibacterium flavum*. *J. Biochem. 68*, 701−710.
(28) Mizukami, T., Hamu, A., Ikeda, M., Oka, T., and Katsumata, R. (1994) Cloning of the ATP phosphoribosyl transferase gene of *Corynebacterium glutamicum* and application of the gene to L-histidine production. *Biosci., Biotechnol., Biochem. 58*, 635−638.
(29) Ohnishi, J., Mitsuhashi, S., Hayashi, M., Ando, S., Yokoi, H., Ochiai, K., and Ikeda, M. (2002) A novel methodology employing *Corynebacterium glutamicum* genome information to generate a new L-lysine-producing mutant. *Appl. Microbiol. Biotechnol. 58*, 217−223.
(30) Cho, Y., Sharma, V., and Sacchettini, J. C. (2003) Crystal structure of ATP phosphoribosyltransferase from *Mycobacterium tuberculosis*. *J. Biol. Chem. 278*, 8333−8339.
(31) Cremer, J., Eggeling, L., and Sahm, H. (1991) Control of the lysine biosynthesis sequence in *Corynebacterium glutamicum* as analyzed by overexpression of the individual corresponding genes. *Appl. Environ. Microbiol. 57*, 1746−1752.
(32) Jetten, M. S., Follettie, M. T., and Sinskey, A. J. (1995) Effect of different levels of aspartokinase on the lysine production by *Corynebacterium lactofermentum*. *Appl. Microbiol. Biotechnol. 43*, 76−82.
(33) Tang, S. Y., and Cirino, P. C. (2011) Design and application of a mevalonate-responsive regulatory protein. *Angew. Chem. 50*, 1084−1086.
(34) Eggeling, L., and Bott, M. (2005) *Handbook of Corynebacterium glutamicum*, CRC Press Taylor & Francis Group, Boca Raton, FL.
(35) Stäbler, N., Oikawa, T., Bott, M., and Eggeling, L. (2011) *Corynebacterium glutamicum* as a host for synthesis and export of D-amino acids. *J. Bacteriol. 193*, 1702−1709.
(36) Bott, M., and Niebisch, A. (2005) *Respiratory Energy Metabolism*, CRC Press Taylor & Francis Group, Boca Raton, FL.
(37) Lausberg, F., Chattopadhyay, A. R., Heyer, A., Eggeling, L., and Freudl, R. (2012) A tetracycline inducible expression vector for *Corynebacterium glutamicum* allowing tightly regulable gene expression. *Plasmid 68*, 142−147.
(38) Huber, R., Ritter, D., Hering, T., Hillmer, A.-K., Kensy, F., Müller, C., Wang, L., and Büchs, J. (2009) Robo-Lector—a novel platform for automated high-throughput cultivations in microtiter plates with high information content. *Microb. Cell Fact. 8*, 42.
(39) Black, S., and Wright, N. G. (1955) beta-Aspartokinase and beta-aspartyl phosphate. *J. Biol. Chem. 213*, 27−38.
(40) Ames, G. F., Noel, K. D., Taber, H., Spudich, E. N., Nikaido, K., and Afong, J. (1977) Fine-structure map of the histidine transport genes in *Salmonella typhimurium*. *J. Bacteriol. 129*, 1289−1297.